EVS30 Symposium
Stuttgart, Germany, October 9 - 11, 2016

Energy Management Optimization Using Predictive Control - A Simulative Study

Julian Eckstein[1], Ulrich Köhler[2], Ludwig Brabetz[3]
[1]*Hella KGaA Hueck & Co., Beckumer Str. 130, 59552 Lippstadt, Germany, julian.eckstein@hella.com*
[2]*Hella KGaA Hueck & Co., Beckumer Str. 130, 59552 Lippstadt, Germany, ulrich.koehler@hella.com*
[3]*University of Kassel, Wilhemshöher Allee 73, 34121 Kassel, Germany, brabetz@uni-kassel.de*

Abstract

Due to rising concerns about internal combustion engines and air quality in urban areas, electric vehicles are considered as a possible solution to overcome these issues. Despite great progress in the field of battery technology, electric ranges are perceived as insufficient. There is only very little surplus energy available to provide comfortable heating, ventilation and air conditioning (HVAC). Next to the drive train as the biggest energy consumer, the HVAC system requires large amounts of energy. Therefore, an energy management system which supervises and controls both major energy consumers was investigated. Model predictive control was chosen as control strategy.

Keywords: BEV (battery electric vehicle), energy consumption, optimization, heating, internal resistance.

1 Introduction

In the near future the total amount of electric vehicles is predicted to increase from 1.3 million in 2015 to more than 30 million in 2025 [1]. Range anxiety is one of the buzzwords which reflect the concerns of many potential buyers of electric vehicles. Especially during cold weather conditions, the already limited electric range is severely reduced since there is no excess heat available from an internal combustion engine. Hence, a comfortable passenger compartment is paid for by a reduction in driving range. In order to ease this predicament an intelligent energy management strategy is favorable to balance consumption, thus enhancing the electric range.
Predictive control offers a way to make the energy management intelligent. Early applications using model predictive control in trucks to reduce fuel consumption were realized in the last decade [2, 3]. For passenger cars promising solutions were published a few years later, mainly dealing with longitudinal vehicle dynamics. Kalabis focused on an efficient automatic cruise control for conventional cars, which resulted in a significant fuel reduction compared to a standard reference scenario [4]. Radke used dynamic programming to solve the arising optimization problems within the model predictive controller [5]. The dynamics of electric vehicles were investigated by Freuer *et al.* [6, 7]. The authors focused on the profound statistical evaluation of test drives. As before, dynamic programming was used as solving method. However, computational demand was shown to be as a serious issue. The computational demand of two predicitive approaches was elaborated in [8]. The authors concluded that a convex cost function outperforms a nonlinear approach in terms of computational demand, for comparable solution quality.
In the field of heating ventilation and air-conditioning (HVAC) electric vehicles represent a new challenge in the automotive sector, as there is no excess heat from an internal combustion engine. The application of electric air heaters, heat pumps and surface/radiation heaters are envisaged as possible solution to

realize a comparable thermal comfort in electric vehicles [9, 10]. Predictive thermal management is discussed with regard to hybrid electric vehicles [11, 12], but it gains more and more interest in the field of electric vehicles as well [13, 14]. However, there are still only very few papers which combine thermal and energy management.
In this paper we propose a predictive controller that acts on the drive train as well as on the HVAC system of an electric vehicle. This paper is structured as follows: In section 2 the vehicle model and the validation process are briefly described. In section 3 a short description of model predictive control is given along with the design of the control strategy. In section 4 the outline of the parameter study is elaborated. The evaluation of the analysis is done in section 5.

2 Modeling

2.1 Vehicle Dynamics

First principles were used to model the longitudinal vehicle dynamics [15]. The resulting model describes the force balance acting on the vehicle:

$$\frac{dv}{dt} = a = \frac{F_d - F_a - F_z - F_r}{m_e}, \tag{1}$$

with actual acceleration a and the equivalent vehicle mass $m_e = m_v e$ which compensates the rotating masses (wheels) by virtually increasing the vehicle mass v by an equivalency factor e. In order to accelerate the vehicle, the drive train force F_d has to overcome the air drag force F_a, the downhill force F_z and the friction force F_r. To make use of a linear model, the vehicle dynamics are reformulated by using a transformation which was proposed in [16] and extended in [4].We formulate the dynamics based on a the path discrete kinetic energy balance:

$$\begin{aligned} & E_{kin}(k+1) = E_{kin}(k) + \Delta E_{kin}(k) \\ \Leftrightarrow \quad & \frac{1}{2} m_e v^2(k+1) = \frac{1}{2} m_e v^2(k) + \left[F_d(k) - F_a(k) - F_z(k) - F_r(k)\right] \Delta s, \end{aligned} \tag{2}$$

where E_{kin} is the kinetic energy of the vehicle, v the vehicle speed and Δs the path discrete step size. The forces can be decomposed into their constituents:

$$\begin{aligned} F_d &= \frac{T}{r}, & F_r &= \mu(m_v + m_a) g\, cos(\alpha), \\ F_a &= \frac{1}{2} \rho c_w A_v v^2, & F_\alpha &= (m_v + m_a) g\, sin(\alpha). \end{aligned} \tag{3}$$

Here, g represents the gravitational constant, T the drive wheel torque, α the inclination of the road, ρ the density of the air, c_w the air drag coefficient, A_v the frontal area of the vehicle, m_a the additional mass (passengers, payload) and μ the rolling friction coefficient. Simplifying $cos(\alpha) = 1$ and $sin(\alpha) = \alpha$ in (3), inserting (3) into equation (2) and rearranging for $v^2(k+1)$ results in

$$v^2(k+1) = A v^2(k) + B_u T(k) + B_\alpha \alpha(k) + b_\mu, \tag{4}$$

where the system matrix A, the input matrix b_u, the disturbance matrix B_α and the friction term b_μ are defined as follows

$$\begin{aligned} A &= 1 - \Delta s \rho c_w A_v / m_e & b_\mu &= -2 \Delta s\; g\; (m_v + m_a)/m_e\; \mu, \\ B_u &= 2 \Delta s / (r m_e), & B_\alpha &= -2 \Delta s\; g\; (m_v + m_a)/m_e. \end{aligned} \tag{5}$$

For further details refer to [4, 16]. Conforming to the common standard we assign the state variable, the input and the disturbance variable as $x := v^2$, $u := T$ and $z := \alpha$. This results in the scalar state space model:

$$x(k+1) = A x(k) + B_u u(k) + B_z z(k) + b_\mu. \tag{6}$$

2.2 Passenger Compartment

The passenger compartment is simulated by the use of a point mass model [17, 18], which takes relevant vehicle parameters into account. These parameters cover the properties of the windows, the chassis as well as environmental conditions and number of passengers. The compartment temperature is the main output parameter. It is used as an indicator of comfort. The inlet air temperature and the inlet air mass flow serve as model inputs. Further environmental parameters, which may change over time, such as solar radiation, wind or vehicle velocity are regarded as disturbances. The states of the model are the temperatures of the compartment air, the windows (sides, rear and front), the interior components, the splash back, the roof, the side elements and the mass of water in the compartment air. We fitted the model with a *Trust-Region Reflective Newton Algorithm* provided by MATLAB to a measurement on a temperature-controlled roller test bench with a typical B-Segment vehicle. The resulting temperatures are depicted in Fig. 1. Taking into account the model complexity, the agreement of simulation and

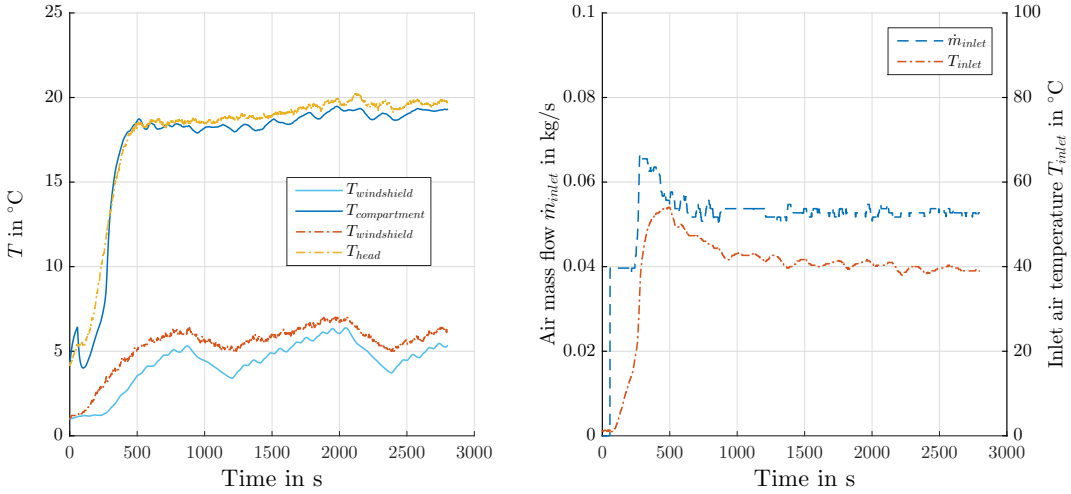

Figure 1: Comparison of temperatures from simulation (filled) and from real measurement (dotted) for validation on the left side and according inputs on the right side.

measurement is acceptable. For more information about the fitting and validation process refer to [19]. In the course of this paper, we will refer to the heat flow into the compartment as HVAC power.

2.3 Drive train and electrical system

The drive train consists of two permanent-magnet synchronous machines which are directly connected to the front wheels. There is one inverter for each motor which is connected to the high voltage bus. A lithium-iron-phosphate traction battery feeds the high voltage bus. The identical motors are modeled with an efficiency map, which already incorporates the inverter losses. The battery model consists of two RC elements, which are parameterized by temperature and state of charge (SOC), based on look-up tables. Conduction losses have been neglected. During validation drives on public streets and on a roller test bench deviations of less than 7 % were achieved [20].

3 Predictive Control

3.1 Concept

Model predictive control (MPC) uses an internal process model to predict future states $x(k+i)$ and outputs $y(k+i)$ of the controlled plant. The required optimal inputs $u(k+i-1)$ are calculated via minimization of a cost function which is commonly of quadratic nature. For a defined prediction horizon H_p with n_p breakpoints, the optimal inputs are calculated by using a quadratic program. However, only the first input value(s) $u(k)$ are applied to the real plant. The next optimization loop is carried out with the new state(s) $x(k+1)$ as initial value [21]. The relation between inputs, states and outputs can be

represented as a linear time-invariant state-space formulation:

$$\begin{aligned} \boldsymbol{x}(k+1) &= \boldsymbol{A}\boldsymbol{x}(k) + \boldsymbol{B}_u\boldsymbol{u}(k) \\ \boldsymbol{y}(k) &= \boldsymbol{C}\boldsymbol{x}(k) + \boldsymbol{D}_u\boldsymbol{u}(k), \end{aligned} \tag{7}$$

where the matrices $\boldsymbol{A}$, $\boldsymbol{B}_u$, $\boldsymbol{C}$ and $\boldsymbol{D_u}$ contain the system, input, output and direct feedthrough characteristics, respectively. By applying (7) recursively, the prediction model can be formed:

$$\boldsymbol{X}(k) = \boldsymbol{\Phi}\boldsymbol{x}(k) + \boldsymbol{\Gamma}_u\boldsymbol{U}(k). \tag{8}$$

The state prediction vector $\boldsymbol{X}$ holds all future states $\boldsymbol{x}(k+i), i = 1 \dots N$ as elements, where N is the number of prediction steps. The input prediction vector $\boldsymbol{U}$ is formed analogously: $\boldsymbol{u}(k+i-1), i = 1 \dots N$. $\boldsymbol{\Phi}$ consists of the elements: $\boldsymbol{\phi_i} = \boldsymbol{A}^i, i = 1 \dots N$. The *toeplitz* matrix $\boldsymbol{\Gamma}_u$ is built up from $[\boldsymbol{B}_u, \boldsymbol{\Phi}(1 \dots N-1)\boldsymbol{B}_u]$ and $[\boldsymbol{B}_u, \boldsymbol{0} \dots \boldsymbol{0}]$ which results in a lower triangular matrix form. Taking the state space model from (6) the prediction model used in this work becomes linear path invariant and results in:

$$\boldsymbol{X}(k) = \boldsymbol{\Phi}x(k) + \boldsymbol{\Gamma}_u\boldsymbol{U}(k) + \boldsymbol{\Gamma}_z\boldsymbol{Z}(k) + \boldsymbol{\Gamma}_\mu\boldsymbol{G}_\mu. \tag{9}$$

The disturbance vector $\boldsymbol{Z}(k)$ are built up analogously to $\boldsymbol{U}(k)$ and toeplitz matrices Γ_z and Γ_μ analogously to $\boldsymbol{\Gamma}_u$ with $\boldsymbol{B}_z$ and $\boldsymbol{1}$ instead of $\boldsymbol{B}_u$, respectively. Furthermore, $\boldsymbol{G}_\mu = [b_\mu \dots b_\mu]^T$.

3.2 Cost function

The design of the cost function has a major impact on the behavior of the controller. This is why it has to be defined carefully. We chose to use a quadratic cost function due to the fact that there exist powerful solving algorithms for convex optimization problems. A typical cost function is the weighted sum of the states and inputs (for simplification we set $\boldsymbol{C} = 1$ and $\boldsymbol{D}_u = 0$, thus $x = y$, this is why we omit the y terms in the following):

$$J(k) = x^2(k) \cdot q(k) + \boldsymbol{X}^T(k)\boldsymbol{\Omega}\boldsymbol{X}(k) + \boldsymbol{U}^T(k)\boldsymbol{\Psi}\boldsymbol{U}(k). \tag{10}$$

The quadratic form of (10) ensures that a global optimum exists when $\boldsymbol{\Omega}$ and $\boldsymbol{\Psi}$ are positive semi-definite. Both matrices have the state weights $q(k+i) > 0$ (respectively, the input weights $r(k+i) > 0$) as only non-zero elements on their main diagonal. The last state weight $q(k+N) = p > 0$ is commonly used to stabilize a finite horizon, i.e. $N \neq \infty$ [21]. The cost function described above will drive the state towards the origin, as the costs are obviously zero at this point. In some cases it is favorable to shift the origin to an arbitrary steady state (ss) value. This can be achieved by setting $x(k+1) = x(k) = x_{ss}$ in (7) and solving for u_{ss}. Both steady state values are used to extend the x and u terms in the form of $x - x_{ss}$. Thus, the same changes occur in the cost function (10). If there are no constraints, the solution can be found analytically. By inserting the prediction vector (9) into the cost function (10), the problem can be reformulated as follows (for legibility we omit the step index k from now on):

$$J = \frac{1}{2}\boldsymbol{U}^T\boldsymbol{H}\boldsymbol{U} + \boldsymbol{f}\boldsymbol{U}^T + g \tag{11}$$

The symmetric matrix H holds all quadratic terms of U, whereas the vector $\boldsymbol{f}$ sums up all linear terms and g all ($\boldsymbol{U}$) independent terms [22]:

$$\begin{aligned} \boldsymbol{H} &= \boldsymbol{\Psi} + \boldsymbol{\Gamma}^T\boldsymbol{\Omega}\boldsymbol{\Gamma} \\ \boldsymbol{f} &= \boldsymbol{F}x + \boldsymbol{F}_x\boldsymbol{X}_s + \boldsymbol{F}_u\boldsymbol{U}_s + \boldsymbol{F}_zZ + \boldsymbol{F}_\mu\boldsymbol{G}_\mu \\ g &= g(x, \boldsymbol{X}_x, \boldsymbol{U}_s, \boldsymbol{Z}, \boldsymbol{G}_\mu), \end{aligned} \tag{12}$$

with

$$\begin{aligned} \boldsymbol{F} &= 2\boldsymbol{\Gamma}^T\boldsymbol{\Omega}\boldsymbol{\Phi}, & \boldsymbol{F}_x &= -2\boldsymbol{\Gamma}^T\boldsymbol{\Omega}, \\ \boldsymbol{F}_z &= 2\boldsymbol{\Gamma}^T\boldsymbol{\Omega}\boldsymbol{\Gamma}_z, & \boldsymbol{F}_u &= -2\boldsymbol{\Psi}, \\ \boldsymbol{F}_\mu &= 2\boldsymbol{\Gamma}^T\boldsymbol{\Omega}\boldsymbol{\Gamma}_\mu, & \boldsymbol{G}_\mu &= [b_\mu \dots b_\mu]^T. \end{aligned} \tag{13}$$

Differentiating (11), setting to zero and solving for $\boldsymbol{U}$ leads to

$$\boldsymbol{U} = -\boldsymbol{H}^{-1}\boldsymbol{f}, \tag{14}$$

which is a global minimum as H is positive semi-definite if $q_i \geq 0$ and $r_i \geq 0$. In the presence of state or input constraints a numerical solver is required. As there are limitations on wheel torque as well as on vehicle velocity, we choose the MATLAB solver "quadprog" which uses the well-known *Interior-Point* algorithm in our case. The aim of our analyses is to reduce the energy consumption. As a side effect we reduce the power loss of the battery (and in the power lines, which is out of the scope of this paper). We achieve this by optimizing the velocity trajectory of the vehicle. However, we cannot optimize the trajectory directly, because the above mentioned scheme deals with the optimization of the wheel torque for a given velocity (state) set point. Thus, at least in steady state, an optimal reference input must be provided. If the track, i.e. the road inclination, is known, the optimal steady state velocity v_{ss} can be calculated by inverting the vehicle model (6). This is similar to the procedure described above to shift the origin. We use the path specific electric energy consumption C_{el} as cost function:

$$\begin{aligned} C_{el} &= \frac{E_{el}}{\Delta s} + \frac{E_{HVAC}}{\Delta s} = \frac{T_{ss}\omega}{\eta \Delta s} t + \frac{P_{HVAC}}{\Delta s} t \\ &= \frac{T_{ss} v_{ss}}{r \eta \Delta s} \frac{\Delta s}{v_{ss}} + \frac{P_{HVAC}}{\Delta s} \frac{\Delta s}{v_{ss}} = \frac{T_{ss}}{r\eta} + \frac{P_{HVAC}}{v_{ss}} \end{aligned} \tag{15}$$

$$\text{with } T_{ss} = u_{ss} = \frac{(1-A)x_{ss} - B_z z - b_\mu}{B_u} \text{ and } v_{ss} = \sqrt{x_{ss}}. \tag{16}$$

We apply the MATLAB optimization solver "fminsearch" and cross check the result with a parameter analysis of v for a given angle z and HVAC power P_{HVAC}. In Fig. 2 the solution surface is displayed. At first glance a symmetric distribution can be observed. Closer inspection reveals that there is an unsteadiness an inclination of about -1.5 degrees. The reason is the zerocrossing of the torque in this area. As a result, the vehicle behavior changes from drive to recuperation. The comparably low efficiency causes the spikes depicted in Fig. 2. By enhancing the state space model with the information of steady

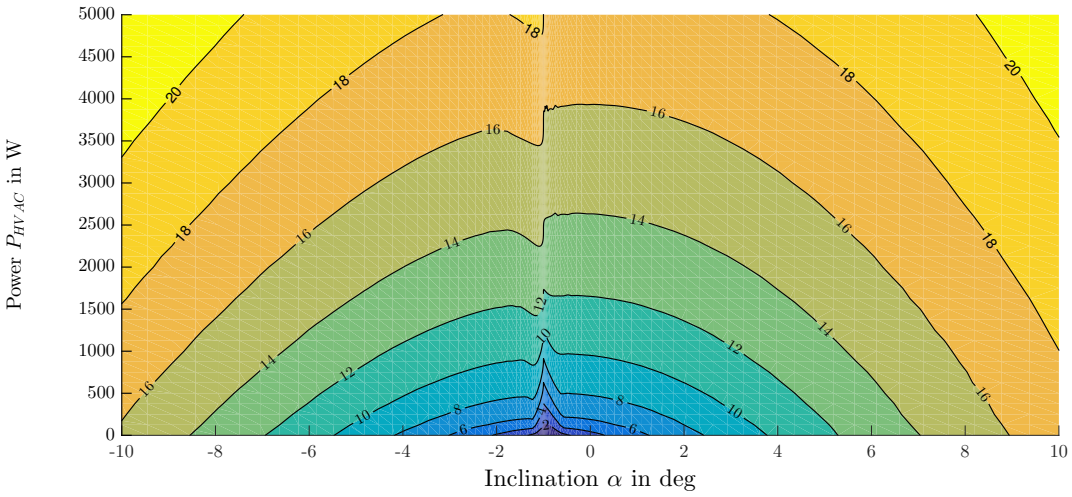

Figure 2: Optimal steady state velocity v_{ss} in m/s in dependence of inclination α and power P_{HVAC}.

state velocity (and torque) the MPC is able to reach an optimal stationary point. However, stationary conditions are only a part of typical driving scenarios. Constant velocity cruising most likely occurs on non-urban roads and motorways, rarely within urban cities due to dense traffic, intersections etc. Thus, a more dynamic, or "transient", behavior of the vehicle is favored to cover further scenarios. Such behavior is achieved by setting $u_{ss} = 0$. This leads to a (minor) steady state error. The two different trajectories are shown in Fig. 3 for a track with an inclination of 3 degrees (analogous to Fig. 5). It can be observed that the stationary cost function leads to a smooth trajectory with neatly s-shaped transitions and a perfect match of precomputed optimal velocity in the steady state sections (i.e. no steady state error). On the other, hand we see a different steady state velocity for the transient cost function and distinct spikes in the trajectory.

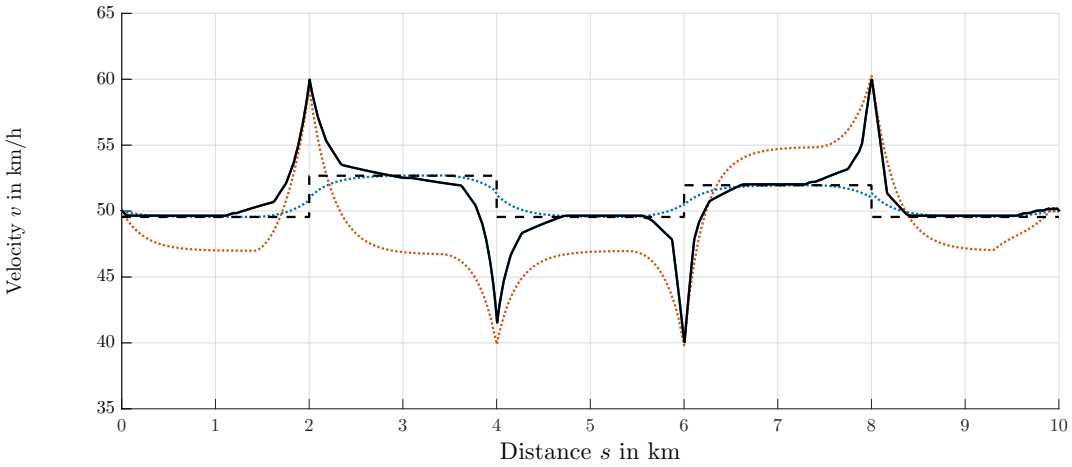

Figure 3: Comparison of both trajectories (transient: dotted-red, stationary: dotted-blue) with the optimal steady state velocity v_{ss} (dashed-black) and global optimal velocity trajectory from DP (filled-black).

3.2.1 Dynamic Programming

When compared to a *Dynamic Programming* (DP) approach, which is used elsewhere [2, 5, 7, 23], it can be observed that neither the transient nor the stationary MPC solution match the global optimal solution. DP is a numeric method to find a global optimal solution. It requires the states, inputs and time/path to be discretized, which has the disadvantage of all numeric approaches that accuracy is paid for by computational effort. Typically, the solution process starts at the end of the problem and then proceeds backwards along the solution space. We apply DP in such a way that the entire track is solved as batch. By doing so, we ensure to find a global solution for the entire track. For further details about DP refer to [24].

3.2.2 Adaptive Cost Function

By comparing the computed trajectory of DP and both MPC approaches (cf. Fig. 4), it can be seen that neither the stationary ($J_{stationary}$) nor the transient ($J_{transient}$) cost function approach can follow the DP trajectory entirely. Thus, the SOC values are both lower. This implies that a fixed cost function is not sufficient here. When looking at the velocity trajectories it is noticeable that there are sections where the transient MPC approach seems to be more suitable and there are sections where the stationary approach appears favorable. Consequently, we create an adaptive cost function $J_{adaptive}$ which is a superposition of both. A parameter γ is used to adjust each contribution:

$$J_{adaptive} = \gamma \cdot J_{stationary} + (1-\gamma) \cdot J_{transient}, \quad \gamma = 0 \ldots 1. \tag{17}$$

The weighting parameter γ has been designed to reflect the optimal steady state velocity v_{ss}, which in turn is a parameter of the environment (here: road inclination z). If a change $|\Delta v_{ss}|$ exceeds a certain threshold, γ is calculated by a bounded affine law. The application of the adaptive cost function to the optimization problem leads to a better fit of DP velocity trajectory and MPC trajectory. Thus, the resulting SOC value is closest to the DP solution.
By plant inversion a look-up table is created which returns the energy optimal velocity for given road and weather conditions. In this way we are able to provide an optimal reference trajectory for steady state operation. By adjusting the weighting factors in the cost function, the controller can be tuned, e.g. to favor higher velocities in order to increase travel time or, on the other hand, reduce energy consumption which in turn results in a range enhancement. To prove the robustness and the validity of such a cost function a simulation study is performed.

3.2.3 Extension of model and cost function

As described before, the HVAC system is one of the main energy consumers in an electric vehicle. Therefore, it is reasonable to include the HVAC control in an energy management optimization. We have already considered a mean HVAC power in the MPC approach described above. In the following step, HVAC power will be included as a control parameter. The HVAC modeling described in section 2.2 deals

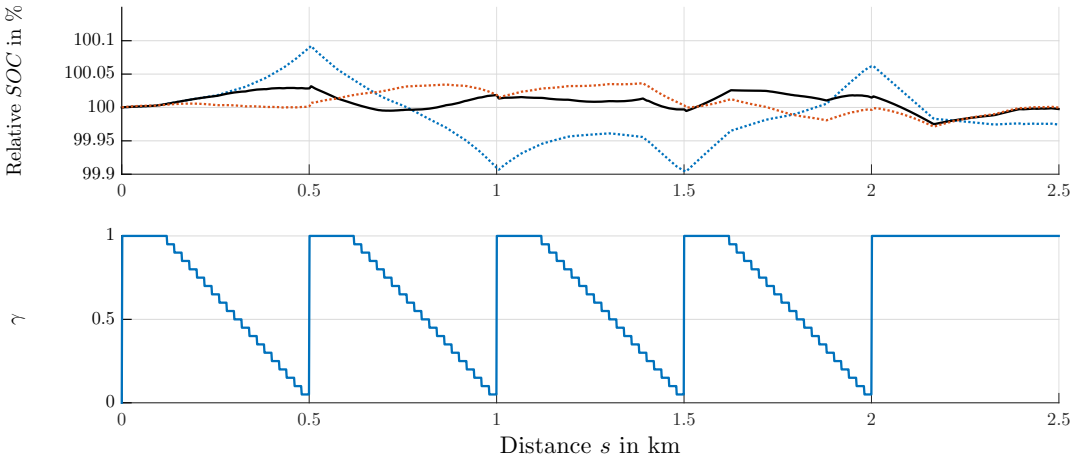

Figure 4: Comparison of relative SOC (top) with respect to DP solution: $SOC_{transient}$ (dotted-red) $SOC_{stationary}$ (dotted-blue) and $SOC_{adaptive}$ (filled-black), weighting factor γ (bottom).

with nine states which would increase the MPC complexity dramatically, thus becoming impractical for the intended application. Nevertheless, it is acceptable to only use the desired HVAC power and the actual (controlled) HVAC power. We extend the state space model (6) by an integrator which accumulates the provided HVAC power. Furthermore, we implement the desired HVAC power as disturbance to the system (similar as in the case of the inclination above). The resulting model becomes

$$\begin{bmatrix} x_1(k+1) \\ x_2(k+1) \end{bmatrix} = \begin{bmatrix} A_1 & 0 \\ 0 & A_2 \end{bmatrix} \begin{bmatrix} x_1(k) \\ x_2(k) \end{bmatrix} + \begin{bmatrix} B_1 & 0 \\ 0 & B_2 \end{bmatrix} \begin{bmatrix} u_1(k) \\ u_2(k) \end{bmatrix} + \begin{bmatrix} B_{1,z} & 0 \\ 0 & B_{2,z} \end{bmatrix} \begin{bmatrix} z_1(k) \\ z_2(k) \end{bmatrix} + \begin{bmatrix} B_{1,\mu} & 0 \\ 0 & 0 \end{bmatrix} \begin{bmatrix} b_{1,\mu} \\ 0 \end{bmatrix}. \tag{18}$$

The index 1 refers to the original system (cf. (6)) whereas index 2 indicates the new state. Here,

$$A_2 = 1 \tag{19}$$

$$B_2 = B_{2,z} = \Delta t, \tag{20}$$

where Δt represents the time step, x_2 the energy divergence, u_2 the delivered power and z_2 the required power for the HVAC system.
The prediction model is extended accordingly. The cost function is extended as well, but up to now both states are completely independent from each other. A typical cost function such as (10) consists of the weighted sums of the squares of the individual states and inputs. However, here we need the square of a summation of states. This can easily be achieved by using a linking matrix $\tilde{E}$. Thus, the symmetric matrix $\tilde{H}$ becomes

$$\tilde{\boldsymbol{H}} = \tilde{\boldsymbol{\Psi}} + \tilde{\boldsymbol{E}}^T \tilde{\boldsymbol{\Gamma}}^T \tilde{\boldsymbol{\Omega}} \tilde{\boldsymbol{\Gamma}} \tilde{\boldsymbol{E}}, \tag{21}$$

where $\tilde{\boldsymbol{E}}$ is a matrix which has the following sub-matrix along its diagonal:

$$\begin{bmatrix} 1 & e_1 \\ e_2 & 1 \end{bmatrix}. \tag{22}$$

For a single step $i \neq N$ in the horizon this gives:

$$j_i = x_1^2 q_1 + x_2^2 q_2 + (u_1 + e_1 u_2)^2 r_1 + (u_1 e_2 + u_2)^2 r_2 \tag{23}$$

The aim is to optimize the input torque (respectively, the velocity) with a high priority, as the drive train is the largest consumer in an electric vehicle. HVAC power optimization is a secondary aim because it is the second highest consumer. This can be achieved by setting $q_1 \gg q_2$. However, we demand that

$x_2 \approx 0$, i.e. at the end of the horizon the provided HVAC energy shall meet the required HVAC energy. A high value p_2 on the final state $x_2(k+N)$ forces this behavior. We choose this option over a hard constraint on the final state to avoid infeasibility problems. Based on observations on the DP solution the state constraints on x_2 are found suitable with ± 50 kJ along the track. Yet, this would not guarantee that the energy difference is near zero at the end of the track. Thus, we narrow the constraints to ± 100 J near the end of the track. A step proved to be suitable, even though a ramp, i.e. a smoother constraint transition, could be beneficial if robustness problems occur.

4 Study

4.1 Scenarios

As the cost function has merely been deduced, a parameter analysis is conducted. We choose to take a simple track consisting of two constant inclination sections and three flat sections in an alternating pattern. This corresponds to drives through a valley or over a hill. In Fig. 5 the five sections are displayed. Here, the main parameters are the inclination angle z and the length of each track. With regard to air-conditioning, we fix the inlet temperature and vary the air mass flow according to the calculated HVAC power. In the present paper we use a stationary state of the passenger compartment model. Furthermore, the model is not used during the optimization process but used to evaluate passenger comfort by means of the passenger compartment air temperature.

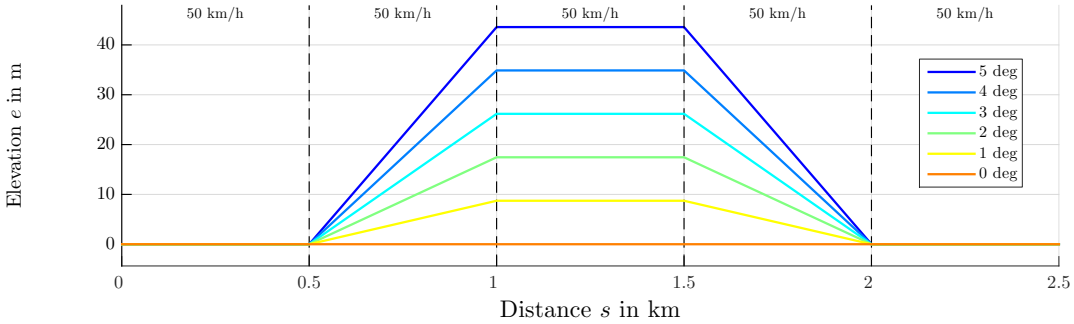

Figure 5: Track elevation profiles for hill drive scenarios.

4.2 Setup

In most approaches, an arbitrary reference velocity is chosen (e.g. in [5, 7, 23]). In contrast we use a precomputed optimal reference and compare it with a global optimal solution. For each scenario, two independent simulations are executed: One utilizes the predictive controller which leads to a suboptimal solution and the other is used as a reference to evaluate the quality of the predictive solution. The reference is calculated with a dynamic programming approach, which is known to find a global optimum of a given optimization problem only limited by discretization and resolution [24]. To ensure comparability of the optimization solutions, the resulting torque and HVAC power trajectories are applied to a sophisticated electric vehicle model (cf. section 2.3), which yields in an SOC value at the end of the track. For each scenario we first apply dynamic programming which we will later use as a reference to compare our MPC results with. We do this stepwise by starting with a velocity trajectory optimization followed by an HVAC optimization. The DP results are applied afterwards on a detailed vehicle dynamics model to calculate reference SOC and travel time. Based on the derived mean velocity and specified (given) HVAC power we run the compartment model until a steady state is reached. The steady state is used as a starting point for the subsequent simulation in which the optimized HVAC power is applied. This is done in such a way that the inlet air temperature is kept constant (i.e. we neglect transient behavior of the HVAC system components at this point). Afterwards we pursue the same steps with the MPC algorithm. Additionally, we simulate the vehicle with (constant) mean velocity which we derive from the DP solution. This is done to show the potential of the proposed strategy. Due to space limitations we only show the results for the inclination angle z as input. The feasible velocity range has been set to 50 km/h with a tolerance of ± 20 %. Furthermore, we set the length of each segment to 500 m and the inlet air temperature is fixed at 25°C. As environmental conditions we set the ambient temperature to 10°C and relative humidity to 45 %. It should be noted that we make sure the energy transfer into the compartment is the same for all scenarios.

5 Results

The resulting input trajectories for the defined scenarios are displayed in Fig. 6. The corresponding state trajectories are visualized in Fig. 7 for a specified HVAC power of 2500 W. When comparing DP

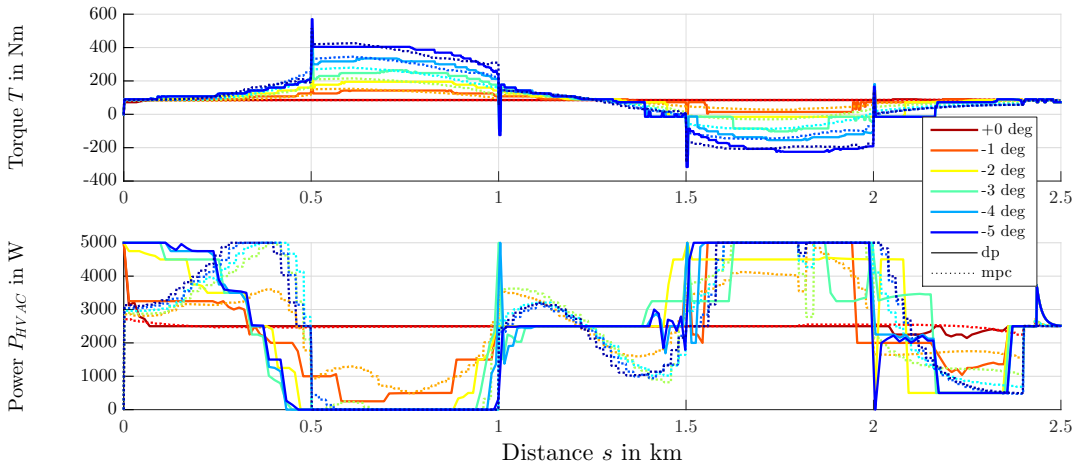

Figure 6: Optimized inputs from DP (filled) and MPC (dotted) for hill drive scenarios.

and MPC torque results, a similar behavior is observed. This is remarkable because two different cost functions and algorithms have been used. So we see a good agreement.

Concerning the HVAC power, certain differences are present. These are most prominent in the first

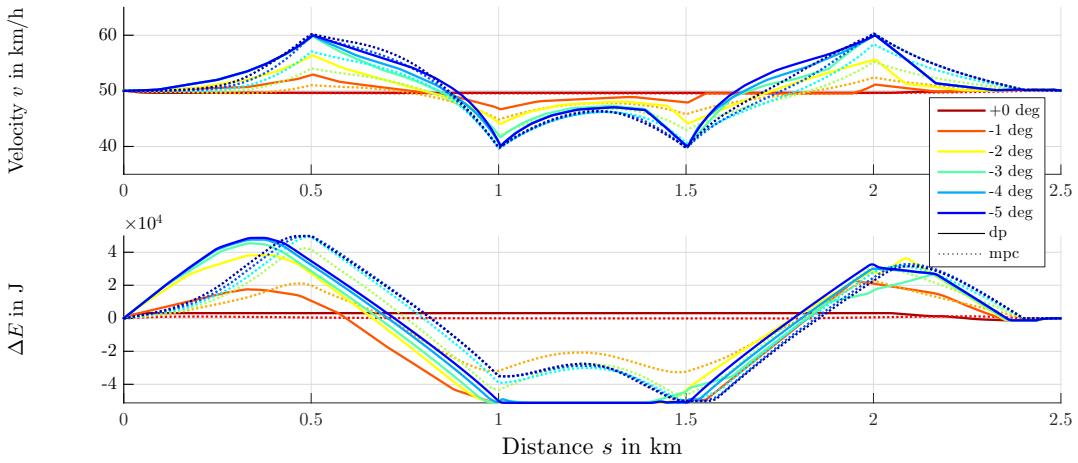

Figure 7: Optimized states from DP (filled) and MPC (dotted) for hill drive scenarios with inclination z as parameter.

section, where DP trajectories are falling whereas MPC trajectories are increasing. This behavior is due to the limited knowledge of the MPC, as it has only a prediction horizon of 600 m. So the trajectories might be different but they are plausible.

When comparing both inputs it can be observed that they are counteracting each other as it was intended, i.e. positions with high torque have a low HVAC power and vice versa.

The velocity trajectories (cf. Fig. 7) prove to have good qualitative agreement and they lack quantitative agreement. This is directly linked to the torque trajectories, thus plausible. Furthermore, it can be seen that the constraints of 40 and 60 km/h are not violated.

The difference in HVAC energy of the MPC follows the DP trajectories with a certain delay at first, which reduces in the course of the track. The main reason for the good agreement near the end is most probably the mutual constraint of having a near zero difference at the end of the track.

From the state and input trajectories it can be concluded that a velocity increase (decrease) is favorable

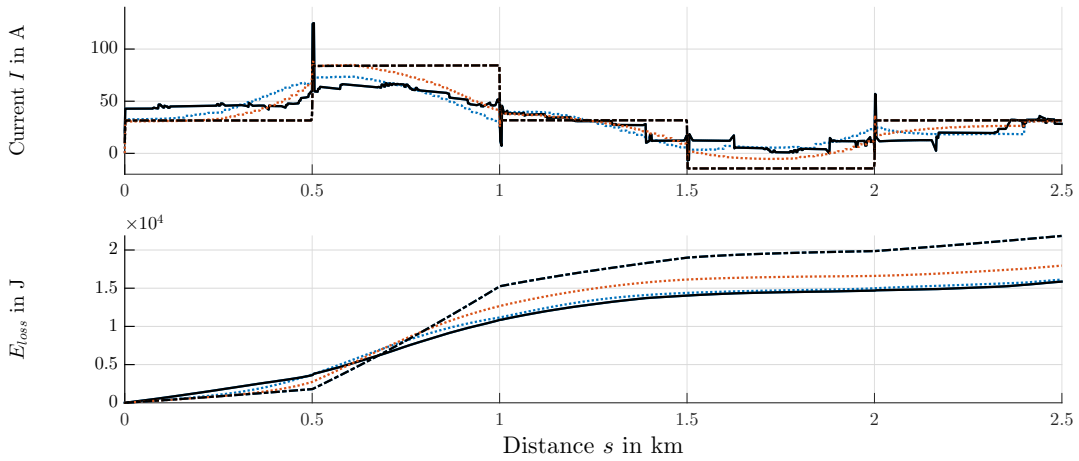

Figure 8: Current (top) and battery loss (bottom) trajectories for a scenario with $z = \pm 3$ degrees. DP (filled-black), mean velocity (dashed-dotted-black), MPC pure velocity optimization (dotted-red) and combined MPC optimization (dotted-blue).

in front of positive (negative) road inclinations. This is in agreement with the literature [7]. Furthermore, a counteraction of the drive train power by the HVAC power seems to be advantageous. The spikes occurring at a change of inclination are simulation artifacts.
In Fig. 8 the current and battery energy loss trajectories for the ± 3 degrees scenario are shown. It is obvious that the DP current trajectory has a far smaller amplitude than the mean velocity trajectory (which has the highest one). Additionally, the MPC results are shown for a pure velocity optimization (cf. Section 3.2) and a combined optimization (cf. Section 3.2.3). The combined MPC approach is closest to the DP current trajectory. This can be seen in the battery loss trajectory as well, especially at the end, where the combined MPC trajectory has the second smallest energy loss. The improvement with respect to the mean velocity battery loss is 17.80 % for the MPC velocity approach, 26.14 % for the combined MPC approach and 27.38 % for the DP approach. The reduction of peaks in the current have a major impact on the battery energy loss because the ohmic loss scales quadratic with the current. A reduced battery current enhances battery lifetime [13] and might allow a certain amount of downsizing (in terms of power) when the proposed approach is used. Since the internal resistance of lithium-ion batteries is very low, the above mentioned improvements do not affect the SOC in the same way. Here, the improvements are 1.31 %, 1.43 % and 1.62 %, respectively. However, the travel times of the MPC approaches are increased by 2.07 % when compared with the DP solution.
It remains to consider the passenger comfort which we do via the compartment air temperature. In Fig. 9 the resulting temperature is shown for the ± 3 degrees scenario. The temperature amplitude is less than 0.3 K which will hardly be noticeable for the passengers. Thus, the comfort is not affected. Concerning

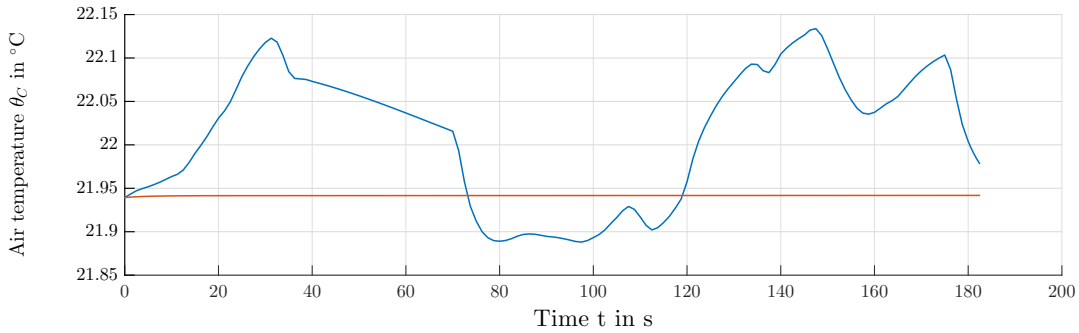

Figure 9: Compartment air temperature for the combined MPC solution (blue) and the pure velocity optimization MPC approach (red).

computing effort, literature states computing times in the order of seconds up to minutes [7, 23], whereas the quadratic optimization of the proposed approach lies in the area of a few milliseconds. However, this depends strongly on discretization, number of inputs, states, constraints and the concrete implementation.

6 Conclusions and Outlook

A model predictive control approach combining a longitudinal dynamics optimization and a passenger compartment air-conditioning optimization has been presented. The structure of the MPC was detailed and justified. The validity and effectiveness has been shown by a comparison with a global dynamic programming approach. Particularly concerning the longitudinal dynamics, it is favorable to increase the velocity in front of a positive road inclination and to decrease the velocity in front of a negative road inclination, this is agreement with literature [7, 20]. The larger the inclination angle, the more energy can be saved compared to a constant velocity. Higher required HVAC power imply higher velocities to reduce travel time.
Concerning the passenger compartment conditioning we could show that redistributing the HVAC power along a given horizon results in a reduction of several tenths of a percent of SOC. This may not have a major impact on the range of vehicles using a high efficient battery chemistry, but it may gain more relevance in the next years. It has to be stated that the range extension potential of the proposed approach in this work falls short compared to the ongoing development in battery chemistry. Nevertheless, the improvements could be achieved by software and it is applicable independent (within certain boundaries) from battery technology and HVAC system design.
The proposed algorithm is a quadratic program which can be solved much faster in comparison with DP approaches, especially when DP is used as solving scheme within an MPC framework.

References

[1] International Energy Agency (IEA). World Energy Outlook 2016 - Executiv Summary. Technical report, International Energy Agency, Paris, 2016.

[2] Stephan Terwen and S. Terwen. *Vorrausschauende Längsregelung schwerer Lastkraftwagen*. 2009. ISBN 9783866444812.

[3] E. Hellström. *Look-ahead Control of Heavy Vehicles*. PhD thesis, Linköping University, 2010.

[4] M. Kalabis. *Steigerung der Energieeffizienz von Kraftfahrzeugen durch modellbasierte prädiktive Geschwindigkeits- und Abstandsregelung*. Dissertation, Technische Universität Kaiserslautern, 2013.

[5] T. Radke. *Energieoptimale Längsführung von Kraftfahrzeugen durch Einsatz vorausschauender Fahrstrategien*. Dissertation, Karlsruher Institut für Technologie (KIT), 2013.

[6] A. Freuer, M. Grimm, and H.-C. Reuss. Automatic cruise control for electric vehicles - Statistical consumption and driver acceptance analysis in a representative test person study on public roads. In , *14. Internationales Stuttgarter Symposium*, Proceedings, pages 759–779, Wiesbaden, 2014. Springer Fachmedien Wiesbaden. ISBN 978-3-658-05129-7.

[7] A. Freuer. *Ein Assistenzsystem für die energetisch optimierte Längsführung eines Elektrofahrzeugs*. Springer Fachmedien Wiesbaden, Wiesbaden, 2016. ISBN 978-3-658-13603-1.

[8] J. Eckstein, K. Schäfer, S. Peitz, P. Friedel, S. Ober-Blöbaum, and M. Dellnitz. A Comparison of two Predictive Approaches to Control the Longitudinal Dynamics of Electric Vehicles. In *3rd International Conference on System-integrated Intelligence: New Challenges for Product and Production Engineering, SysInt 2016*, 2016.

[9] A. Wiebelt and M. Wawzyniak. Thermal Management for Electrified Vehicles. *MTZ worldwide*, 77(5):38–43, 2016.

[10] M. Jung, A. Kemle, T. Strauss, and M. Wawzyniak. Interior Heating for Hybrid and Electric Vehicles. *ATZ worldwide eMagazine*, 113(05):36–40, 2011.

[11] H. Esen, T. Tashiro, D. Bernardini, and A. Bemporad. Cabin Heat Thermal Management in Hybrid Vehicles using Model Predictive Control. In *22nd Mediterranean Conference on Control and Automation (MED)*, 2014. ISBN 9781479959013.

[12] C. Schröder and P. Petr. Nonlinear Model Predictive Control for Thermal and Electrical Power Management for Parallel Hybrid Electric Vehicles. In *Hybrid and Electric Vehicles 11th Symposium*, Braunschweig, 2014. Intelligente Transport- und Verkehrssysteme und -dienste Niedersachsen e.V.

[13] M. A. Al Faruque and K. Vatanparvar. Modeling, analysis, and optimization of Electric Vehicle HVAC systems. In *2016 21st Asia and South Pacific Design Automation Conference (ASP-DAC)*, pages 423–428. IEEE, jan 2016. ISBN 978-1-4673-9569-4.

[14] M. Auer, J. Wiedemann, N. Widdecke, and T. Kuthada. Increase in range of a battery electric vehicle by means of predictive thermal management. In *15th Stuttgart International Symposium*, pages 1495–1508, 2015.

[15] L. Guzzella and A. Sciarretta. *Vehicle Propulsion Systems*. Springer Berlin Heidelberg, Berlin, Heidelberg, 2013. ISBN 978-3-642-35912-5.

[16] N. Kohut. Integrating Traffic Data and Model Predictive Control to Improve Fuel Economy. In , *12th IFAC Symposium on Control in Transportation Systems*, pages 155–160, sep 2009.

[17] J. Eckstein, F. Brunstein, C. Lüke, P. Friedel, and A. Trächtler. A Novel Approach Using Model Predictive Control to Enhance the Range of Electric Vehicles. In *3rd International Conference on System-integrated Intelligence: New Challenges for Product and Production Engineering, SysInt 2016*, 2016.

[18] M. Konz, N. Lemke, S. Försterling, and M. Egthessad. FAT 233: Spezifische Anforderungen an das Heiz-Klimasystem elektromotorisch angetriebener Fahrzeuge, 2011.

[19] J. Tönnishoff. *Synthese und Analyse einer Modellprädiktiven Regelung zur Erhöhung der Reichweite von Elektrofahrzeugen*. Master thesis, University of Paderborn, 2016.

[20] M. Dellnitz, J. Eckstein, K. Flaßkamp, P. Friedel, C. Horenkamp, U. Köhler, S. Ober-Blöbaum, S. Peitz, and S. Tiemeyer. Development of an Intelligent Cruise Control Using Optimal Control Methods. In *International Conference on System-integrated Intelligence SysInt*, volume 15, pages 285–294, Bremen, 2014.

[21] J. M. Maciejowski. *Predictive Control: With Constraints*. Prentice Hall, 2002. ISBN 0201398230.

[22] D. Görges. Relations between Model Predictive Control and Reinforcement Learning. In *Accepted for the Proceedings of the IFAC 2017 World Congress*, Toulouse, France, 2017.

[23] S. F. Gausemeier. *Ein Fahrerassistenzsystem zur prädiktiven Planung energie- und zeitoptimaler Geschwindigkeitsprofile mittels Mehrzieloptimierung*. PhD thesis, Universität Paderborn, 2013.

[24] R. E. Bellmann. *Dynamic Programming*. Princeton University Press, Princeton, 1957.

[25] A. Freuer, M. Grimm, and H.-C. Reuss. Messung und statistische Analyse der Leistungsflüsse und Energieverbräuche bei Elektrofahrzeugen im kundenrelevanten Fahrbetrieb. In *4. Deutscher Elektro-Mobil Kongress*, Essen, 2012.

Authors

M. Sc. Julian Eckstein studied renewable energies at the University of Applied Sciences Nordhausen, where he got his Bachelor's degree. In 2012 he graduated from the University of Aachen, with a Master's degree in the field of energy systems. After working as a research assistant at the Solar Intitute Jülich he entered the automotive industry in 2013 as Ph.D student at HELLA to work on the range enhancement of electrical vehicles. He focuses on predictive control strategies to optimimize the overall energy management of electric vehicles. Within the publicly funded project *ReelaF* he took responsibility for the intelligent energy management system.

Dr. rer. nat. Ulrich Köhler studied physics in Jena, Paderborn and, as a Fulbright scholar, in Ames, IA, USA. There he graduated as M.S. in physics from Iowa State University in 1995. He received his Ph.D. in Physics from Paderborn University in 2003 for research work on cubic Gallium Nitride structures. In 2002 Mr. Köhler joined HELLA's corporate R&D department in Lippstadt, Germany. There among others he is responsible for coordinating public funded research.

Professor Dr. rer. nat. Ludwig Brabetz graduated in physiscs at the University of Münster and received his Ph.D from the University of Siegen. Since 2007 he is chair of vehicle systems and basics of electric engineering at the University of Kassel. He focusses his research on electric energy in vehicles. Before that, Prof. Brabetz had a leading position in the automotive industry in the field of R&D for more than 20 years.